CHEMISTRY OF MATERIALS

COMMUNICATION

pubs.acs.org/cm

Evidence for (Bi,Pb)−O Covalency in the High T_C Ferroelectric $PbTiO_3$−$BiFeO_3$ with Large Tetragonality

Masatomo Yashima,*[,†,‡] Kazuki Omoto,[‡] Jun Chen,*[,§] Hiroki Kato,[‡] and Xianran Xing[§]

[†]Department of Chemistry and Materials Science, Graduate School of Science and Engineering, Tokyo Institute of Technology, 2-12-1-W4-17, O-okayama, Meguro-ku, Tokyo, 152-8551, Japan

[‡]Department of Materials Science and Engineering, Interdisciplinary Graduate School of Science and Engineering, Tokyo Institute of Technology, Nagatsuta-cho 4259, Midori-ku, Yokohama, 226-8502, Japan

[§]Department of Physical Chemistry, University of Science and Technology Beijing, Beijing 100083, China

Supporting Information

KEYWORDS: $BiFeO_3$, $PbTiO_3$, ferroelectric, piezoelectric, crystal structure, electron density, synchrotron, diffraction, Rietveld, maximum-entropy method, first principles, perovskite, lead titanate

Origin of ferroelectricity in $PbTiO_3$ and $BaTiO_3$ has been studied by first-principles calculations and synchrotron X-ray diffraction experiments.[1,2] It was pointed out that the hybridization between the Ti(3d) and O(2p) states is important for the ferroelectric instability in both $PbTiO_3$ and $BaTiO_3$, and that the orbital hybridization exists between the Pb(6s) and O(2p) states to play a crucial role for larger ferroelectricity in tetragonal $PbTiO_3$, whereas the chemical bonding between Ba and O is almost ionic.

In recent years, $PbTiO_3$−Bi*Me*O_3 ferroelectrics have received much attention due to their excellent piezoelectric properties and potential application in high-temperature piezoelectricity (*Me* = Fe, Sc, ($Mg_{0.5}Ti_{0.5}$), etc.).[3−16] The Bi substitution for Pb in $PbTiO_3$ considerably increases both Curie temperature (T_C) and axial ratio c/a.[10−15] The tetragonal 0.4 $PbTiO_3$−0.6 $BiFeO_3$ (Hereafter called as PTBF) exhibits excellent piezoelectric properties, extremely large tetragonality (c/a = 1.16−1.17) and high ferroelectric-paraelectric transition temperature (T_C = 865−874 K).[11−15] However, the role of Bi substitution and origin of the large c/a, high T_C, and ferroelectricity in PTBF are unclear. Furthermore the chemical bonding of PTBF has not been reported yet, which would be a key to solve these unresolved issues.

The purpose of this work is to investigate the chemical bonding in PTBF through synchrotron X-ray diffraction experiments and first-principles calculations. Here we show a strong hybridization between (Bi,Pb)(6s,6p) and O(2p) orbitals in PTBF. Furthermore, we demonstrate that the hybridization between Bi(6s,6p) and O(2p) orbitals is stronger than that between Pb(6s,6p) and O(2p) ones, which is responsible for the enhancement of ferroelectricity by the Bi substitution for Pb in $PbTiO_3$.

PTBF powders were prepared by a sol−gel method and then sintered at 1050 °C. This sintered material was crushed and ground, and then annealed at 800 °C to reduce strains. The PTBF sample thus obtained was identified to be a tetragonal *P*4*mm* perovskite phase by conventional X-ray diffraction measurements, which is consistent with the literature.[11−16] Variable-temperature synchrotron X-ray powder diffraction measurements were performed on the Debye−Scherrer camera with an imaging plate as a detector[17] installed at BL02B2 experimental station of the SPring-8, Hyogo Japan. The powdered PTBF sample was put into a glass capillary tube of 0.1 mm inner diameter. The wavelength of incident beam was determined to be 0.39920 Å using a standard reference material National Institute of Science and Technology (NIST) ceria powders.

Diffraction data were collected at 303.4 and 1000 K in the range from 2θ = 1.3−75°. The temperature of the specimen was controlled by a high-temperature N_2 gas flow system within 0.5 K during each data collection. To obtain experimental electron-density distribution and to refine the structure of PTBF, the synchrotron-diffraction data were analyzed by the maximum-entropy method (MEM) combined with Rietveld refinement using computer programs RIETAN-FP and PRIMA.[18−21] To investigate the electronic structure, we relaxed the atomic positions of an approximated 3 × 2 × 2 supercell of PTBF, antiferromagnetic $Pb_4Bi_8Ti_4Fe_8O_{36}$, on the basis of the density functional theory (DFT) with a program vasp[22] where the unit-cell parameters were fixed to the values obtained in the Rietveld analysis of PTBF (see the details and Figure S1 in the Supporting Information A). The structure and electron-density distribution were drawn by VESTA.[23] As references, the valence-electron-density distributions of metastable antiferromagnetic *P*4*mm* $BiFeO_3$ and stable *P*4*mm* $PbTiO_3$ were also obtained through DFT calculations.

Rietveld refinements of the synchrotron diffraction data of PTBF at 303.4 and 1000 K were successfully performed on the basis of the tetragonal *P*4*mm* and cubic $Pm\bar{3}m$ perovskite-type structures, respectively (Figure 1, Table S1 in the Supporting Information B). The weighted reliability (R) factors in the Rietveld analysis of PTBF at 303.4 and 1000 K were R_{wp} = 6.67% and R_{wp} = 2.77%, respectively. The R factors based on the Bragg intensity and structure factors were R_B = 3.44% and R_F = 1.93%, respectively, for the data at 303.4 K. The R_B and R_F were

Received: April 26, 2011
Revised: June 7, 2011
Published: June 14, 2011

1.99% and 1.92%, respectively, for the data at 1000 K. The refined unit-cell parameters of tetragonal PTBF at 303.4 K were $a = b = 3.83042(5)$ Å and $c = 4.46911(6)$ Å. Thus, the PTBF has an extremely large tetragonality of $c/a = 1.16674(3)$ at 303.4 K,

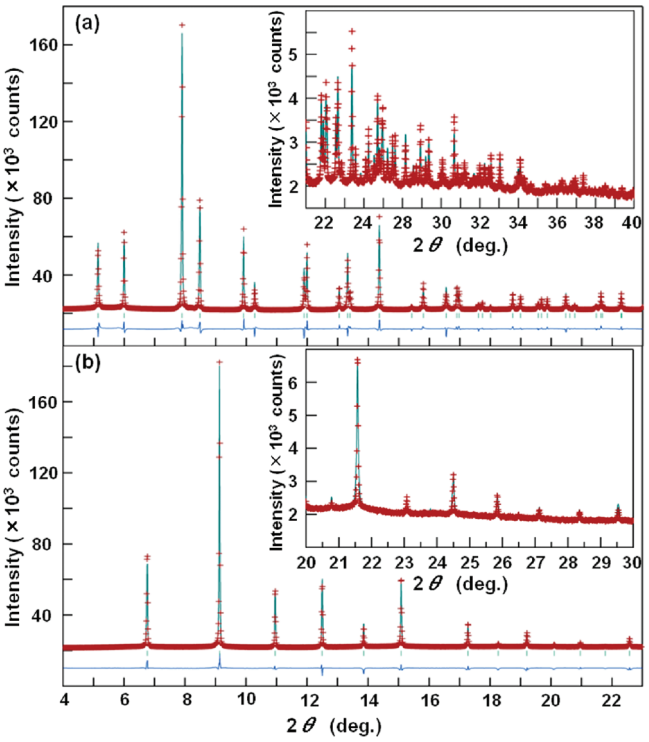

Figure 1. Rietveld fitting patterns of synchrotron powder diffraction data of (a) tetragonal ferroelectric and (b) cubic paraelectric 0.4 $PbTiO_3$–0.6 $BiFeO_3$ at (a) 303.4 and (b) 1000 K. Wavelength of synchrotron X-ray was 0.39920 Å. The high-angular region is enlarged and shown in the insets.

which agrees with those reported in the literature ($c/a = 1.16$–1.17).[11−15] In cubic PTBF, the (Bi,Pb)−O and (Fe,Ti)−O bond lengths are 2.825 and 2.000 Å, respectively. In tetragonal PTBF, the constituent atoms are displaced along the c axis, which yields shorter and longer bond lengths (2.396−3.584 Å for (Bi,Pb)−O bond and 1.591−2.878 Å for (Fe,Ti)−O bond).

Figure 2a−d and Figure S2 in the Supporting Information C show the experimental MEM electron-density distributions of the PTBF. The experimental electron-density distributions on the bc planes at $x = 1/2$ and $x = 0$ ((Bi,Pb)-O planes) of PTBF at 1000 and 303.4 K are shown in panel a and c in Figure 2, respectively. The shorter (Bi,Pb)−O2 bond of tetragonal PTBF at 303.4 K is covalent (A−O2 bond in Figure 2c), while (Bi,Pb)−O bond of cubic PTBF at 1000 K is more ionic (A−O bond in Figure 2a). The (Bi,Pb)−O2 covalent bond in tetragonal PTBF is the experimental evidence for the hybridization of (Bi,Pb)(6s,6p) and O(2p) orbitals (see the partial density of states (DOS) in Figure S3 of Supporting Information D). The electron density distributions in the present PTBF is similar with those in $PbTiO_3$.[2] It should be noted that the (Bi,Pb)-O2 covalent bond (Minimum electron density (MED) = 0.61 $Å^{-3}$) is stronger than Pb−O2 bond in $PbTiO_3$ (MED = 0.45 $Å^{-3}$),[2] which is responsible for the enhancement of ferroelectricity and the increase of T_C and tetragonality by the Bi substitution for Pb in $PbTiO_3$.

Figure 2e shows the corresponding theoretical valence electron-density distribution on the bc plane at $x = 2/3$ of an approximated 3 × 2 × 2 tetragonal supercell of PTBF, $Pb_4Bi_8Ti_4Fe_8O_{36}$, which also indicates the covalent (Bi,Pb)-O bonds. The electron density-of-states of $Pb_4Bi_8Ti_4Fe_8O_{36}$ show that the (Bi,Pb)−O covalent bonds are formed by the overlaps of (Bi,Pb)(6s,6p) and O(2p) orbitals (see Figure S3 of Supporting Information D). It should be noted that the MED at Bi−O bond is higher than MED at the Pb−O bond (Figure 2e). The theoretical MED at the (Bi,Pb)−O2 bond in $Pb_4Bi_8Ti_4Fe_8O_{36}$ is higher than that at the Pb−O2 bond in $PbTiO_3$, which is

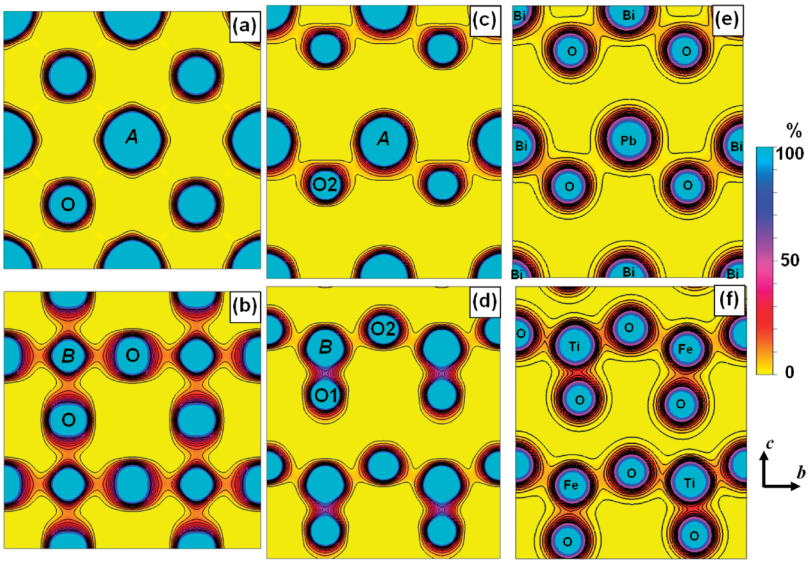

Figure 2. Electron density distributions on the bc planes ((a) $x = 1/2$, (b) $x = 0$) of cubic paraelectric 0.4 $PbTiO_3$-0.6 $BiFeO_3$ (PTBF) from synchrotron data measured at 1000 K. Electron density distributions on the bc planes ((c) $x = 0$, (d) $x = 1/2$) of tetragonal ferroelectric PTBF from synchrotron data measured at 303.4 K. Valence electron density distributions on the bc planes ((e) $x = 2/3$, (f) $x = 1/6$) of $Pb_4Bi_8Ti_4Fe_8O_{36}$ through first-principles calculations. The 0 and 100% in color scale correspond to 0.57 and 4.57 $Å^{-3}$, respectively, in a−d. Contours from 0.57 to 2.57 $Å^{-3}$ by 0.2 $Å^{-3}$ step in a−d. The 0 and 100% in color scale correspond to 0.2 and 4 $Å^{-3}$, respectively, in e and f. Contours from 0.2 to 2 $Å^{-3}$ by 0.2 $Å^{-3}$ step in e and f.

dx.doi.org/10.1021/cm201184y |Chem. Mater. 2011, 23, 3135–3137

consistent with the present experimental results on PTBF. Therefore, the hybridization between Bi(6s,6p) and O(2p) orbitals is stronger than that between Pb(6s,6p) and O(2p) ones, which is responsible for the enhancement of ferroelectricity and the increase of T_C and tetragonality by the Bi substitution for Pb in $PbTiO_3$. The present theoretical MED at the Bi−O bond in *P*4*mm* $BiFeO_3$ (0.50 $Å^{-3}$) is high as well as that in PTBF (average value =0.44 $Å^{-3}$) compared with the theoretical MED at the Pb−O bond in $PbTiO_3$ (0.29 $Å^{-3}$), which is consistent with the large ferroelectric polarization in *P*4*mm* $BiFeO_3$.[24,25]

Covalent (Fe,Ti)−O bonds are observed in panels b and d in Figure 2 and Figure S2 in the Supporting Information C, which is the experimental evidence for the hybridization between (Fe, Ti)(3d) and O(2p) orbitals (see Figure S4 in Supporting Information E). Coordination number of an Fe,Ti atom is six in both tetragonal and cubic PTBF. In cubic PTBF at 1000 K, the MEM electron densities at the six (Fe,Ti)−O bonds are equivalent where the MED at the (Fe,Ti)−O bond is estimated to be 0.85 $Å^{-3}$ (Figure 2b and Figure S2a in the Supporting Information C). On the contrary, in the tetragonal PTBF at 303.4 K, the electron density around an (Fe,Ti) atom is highly anisotropic, which is attributable to the existence of shorter and longer (Fe,Ti)−O bonds. The MED at (Fe,Ti)-O1 bond of tetragonal PTBF (303.4 K) is extremely high (2.3 $Å^{-3}$) indicating high covalency, because the (Fe,Ti)-O1 bond length is short (1.591 Å). The MED at the longer (Fe,Ti)−O2 bond (1.989 Å) is lower (0.66 $Å^{-3}$). It is interesting to point out that the MED at (Fe,Ti)−O bond in PTBF (2.3 $Å^{-3}$) is higher than that at Ti−O bond in $PbTiO_3$ (1.25 $Å^{-3}$).[2] The DFT-based valence electron density of tetragonal $Pb_4Bi_8Ti_4Fe_8O_{36}$ also indicates the Fe−O and Ti−O covalent bonds (Figure 2f). Theoretical density map (Figure 2f) also demonstrates that the covalency of shorter (Fe,Ti)−O1 bond is considerably higher than those of others, which is consistent with the experimental density distribution (Figure 2d). The strong (Fe,Ti)−O1 covalency would also be a key factor for the enhancement of ferroelectricity and the increase of T_C and tetragonality by the Bi substitution for Pb in $PbTiO_3$.

In conclusion, we have successfully addressed the important issue on the chemical bonding of high T_C ferroelectric $PbTiO_3$−$BiFeO_3$ with extremely large tetragonality. The MEM analyses of synchrotron diffraction data of PTBF and first-principles DFT calculations allow us to reliably determine the electron-density distribution of PTBF. In ferroelectric tetragonal PTBF, we have demonstrated the experimental and theoretical evidence for the hybridization between (Bi,Pb)(6s,6p) and O(2p) orbitals, which is the key for the extremely large tetragonality, high T_C and ferroelectricity of PTBF. The (Fe,Ti)-O1 hybridization accompanying with strong covalency would also be a factor for the ferroelectricity of PTBF. Our findings will be favored for the understanding of the physical and chemical properties of $PbTiO_3$−$BiMeO_3$ and for the design of $PbTiO_3$−$BiMeO_3$-based piezoelectric materials (*Me* = Fe, Sc, $(Mg_{0.5}Ti_{0.5})$, etc.).

■ ASSOCIATED CONTENT

Supporting Information. Details of DFT calculations, crystallographic data, and electron-density map and density-of-states. This material is available free of charge via the Internet at http://pubs.acs.org.

■ ACKNOWLEDGMENT

We thank Dr. K. Itoh, Dr. J. Kim, Dr. N. Tsuji, Ms. Y.-C. Chen, Mr. D. Sato, Mr. Y. Yonehara, Mr. U. Fumi, and Mr. S. Matsuyama for their assistance in the synchrotron-diffraction experiments. This research work was partly financially supported by Grant-in-Aids for Scientific Research (B) and Challenging Exploratory Research (21360318, 23655190) from the Ministry of Education, Culture, Sports, Science and Technology of Japan and by the National Natural Science Foundation of China (20731001, 50725415, 91022016). The synchrotron experiments were done at the BL02B2 beamline under the project Nos. 2010B1788 and 2011A11442.

■ REFERENCES

(1) Cohen, R. E. *Nature (London)* **1992**, *358*, 136−138.
(2) Kuroiwa, Y.; Aoyagi, S.; Sawada, A.; Harada, J.; Nishibori, E.; Takata, M.; Sakata, M. *Phys. Rev. Lett.* **2001**, *87*, 217601−1−4.
(3) Kim, J. S.; Cheon, C. I.; Choi, Y. N.; Jang, P. W. *J. Appl. Phys.* **2003**, *93*, 9263−9270.
(4) Cheng, J.-R.; Li, N.; Cross, L. E. *J. Appl. Phys.* **2003**, *94*, 5153−5157.
(5) Zhu, W. M.; Ye, Z.-G. *Ceram. Int.* **2004**, *30*, 1435−1442.
(6) Comyn, T. P.; McBride, S. P.; Bell, A. J. *Mater. Lett.* **2004**, *58*, 3844−3846.
(7) Comyn, T. P.; Stevenson, T.; Bell, A. J. *J. Phys. IV* **2005**, *128*, 13−17.
(8) Chen, J.; Tan, X.; Jo, W.; Rödel, J. *J. Appl. Phys.* **2009**, *106*, 34109−1−7.
(9) Chen, J.; Nittala, K.; Jones, J. L.; Hu, P.; Xing, X. *Appl. Phys. Lett.* **2010**, *96*, 252908−1−3.
(10) Freitas, V. F.; Santos, I. A.; Botero, E.; Fraygola, B. M.; Garcia, D.; Eiras, J. A. *J. Am. Ceram. Soc.* **2011**, *94*, 754−758.
(11) Sunder, V. V. S. S. S.; Halliyal, A.; Umarji, A. M. *J. Mater. Res.* **1995**, *10*, 1301−1306.
(12) Chen, J.; Xing, X. R.; Liu, G. R.; Li, J. H.; Liu, Y. T. *Appl. Phys. Lett.* **2006**, *89*, 101914−1−3.
(13) Bhattacharjee, S.; Tripathi, S.; Pandey, D. *Appl. Phys. Lett.* **2007**, *91*, 042903−1−3.
(14) Zhu, W.-M.; Guo, H.-Y.; Ye, Z.-G. *Phys. Rev. B* **2008**, *78*, 014401−1−10.
(15) Bhattacharjee, S.; Pandey, D. *J. Appl. Phys.* **2010**, *107*, 124112−1−11.
(16) Woodward, D. I.; Reaney, I. M.; Eitel, R. E.; Randall, C. A. *J. Appl. Phys.* **2003**, *94*, 3313−3318.
(17) Nishibori, E.; Takata, M.; Kato, K.; Sakata, M.; Kubota, Y.; Aoyagi, S.; Kuroiwa, Y.; Yamakata, M.; Ikeda, N. *Nucl. Instrum. Methods Phys. Res., Sect. A* **2001**, *467−468*, 1045−1048.
(18) Izumi, F.; Momma, K. *Solid State Phenomena* **2007**, *130*, 15−20.
(19) Izumi, F.; Dilanian, R. A. *Recent Research Developments in Physics,* Vol. 3, Part II; Trivandrum: Transworld Research Network, 2002; pp 699−726.
(20) Yashima, M.; Sirikanda, N.; Ishihara, T. *J. Am. Chem. Soc.* **2010**, *132*, 2385−2392.
(21) Yashima, M.; Saito, M.; Nakano, H.; Takata, T.; Ogisu, K.; Domen, K. *Chem. Commun.* **2010**, *46*, 4704−4706.
(22) Kresse, G.; Joubert, D. *Phys. Rev. B* **1999**, *59*, 1758−1775.
(23) Momma, K.; Izumi, F. *J. Appl. Crystallogr.* **2008**, *41*, 653−658.
(24) Wang, J.; et al. *Science* **2003**, *299*, 1719−1722.
(25) Yun, K. Y.; Ricinschi, D.; Kanashima, T.; Noda, M.; Okuyama, M. *Jpn. J. Appl. Phys.* **2004**, *43*, L647−L648.

■ NOTE ADDED AFTER ASAP PUBLICATION

Published ASAP on 6/14/2011. Version published 7/5/2011 includes change to Acknowledgement.